

UniST: Towards Unifying Saliency Transformer for Video Saliency Prediction and Detection

Junwen Xiong^{1*}, Peng Zhang^{1,2*†}, Chuanyue Li^{1*},
Wei Huang³, Yufei Zha^{1,2}, Tao You¹

¹Northwestern Polytechnical University, ²Ningbo Institute of Northwestern Polytechnical University
³Nanchang University

wshzxjw@mail.nwpu.edu.cn, zh0036ng@nwpu.edu.cn

Abstract

Video saliency prediction and detection are thriving research domains that enable computers to simulate the distribution of visual attention akin to how humans perceiving dynamic scenes. While many approaches have crafted task-specific training paradigms for either video saliency prediction or video salient object detection tasks, few attention has been devoted to devising a generalized saliency modeling framework that seamlessly bridges both these distinct tasks. In this study, we introduce the **Unified Saliency Transformer (UniST)** framework, which comprehensively utilizes the essential attributes of video saliency prediction and video salient object detection. In addition to extracting representations of frame sequences, a saliency-aware transformer is designed to learn the spatio-temporal representations at progressively increased resolutions, while incorporating effective cross-scale saliency information to produce a robust representation. Furthermore, a task-specific decoder is proposed to perform the final prediction for each task. To the best of our knowledge, this is the first work that explores designing a transformer structure for both saliency modeling tasks. Convincible experiments demonstrate that the proposed **UniST** achieves superior performance across seven challenging benchmarks for two tasks, and significantly outperforms the other state-of-the-art methods.

Introduction

As the continuous emergence of massive dynamic data propels deep learning further towards human vision, a growing attention of research has focused on video saliency prediction (VSP) (Bak et al. 2018; Wang et al. 2018a; Tsiami, Koutras, and Maragos 2020) and video salient object detection (VSOD) (Mei et al. 2021; Zhang et al. 2021; Liu et al. 2022a), which are regarded as the fundamental tasks in computer vision. Both the tasks essentially aim to simulate the visual attention distribution of humans perceiving dynamic scenes by modeling spatio-temporal cues in video content. However, the modeling paradigms of prior works are tailored for specialized tasks, and thereby lack the capacity for generalization to address broader tasks.

*These authors contributed equally.

†Corresponding author.

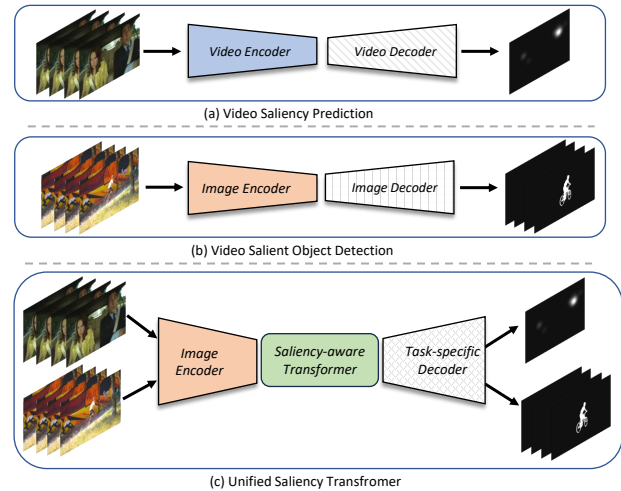


Figure 1: Comparisons of the traditional different modeling paradigm for VSP and VSOD tasks, as well as our proposed unified saliency transformer framework. The VSP and VSOD adopt video encoder and image encoder respectively as feature extractors, followed by corresponding decoders. Differently, a unified saliency transformer directly applies an image encoder for feature processing, and follows a transformer structure for spatio-temporal modeling, and finally uses different decoders for different tasks.

Previous VSP approaches have made impressive progress in predicting the most salient visual regions within frame sequences based on video encoder and decoder (Tsiami, Koutras, and Maragos 2020; Jain et al. 2021; Zhou et al. 2023; Xiong et al. 2023), as depicted in Figure 1(a). To capture spatio-temporal information from video sequences, these methods uniformly rely on video models pre-trained on extensive video datasets, e.g., the lightweight *S3D* (Xie et al. 2018) and the effective *Video Swin Transformer* (Liu et al. 2022b). Subsequently, various kinds of decoding strategies have been successively proposed for processing the obtained spatio-temporal features. (Min and Corso 2019; Jain et al. 2021) proposed a 3D fully convolutional decoder with U-Net-like structure to progressively concatenate features along the temporal dimension. In addition, (Zhou et al.

2023) proposed a 3D convolutional decoder based on the feature pyramid structure, to build high-level semantic features at all scales.

Compared to VSP, the video dataset used in the current VSOD task is usually limited-sized, making it difficult to converge the video encoder-based method to the optimum (Le and Sugimoto 2017; Fan et al. 2019). As a result, many VSOD approaches adopt an image encoder and decoder-based training paradigm, where pre-training is initially performed on the image dataset, and then the pre-trained weights are transferred to the video dataset to further improve the model’s generalization capabilities (Gu et al. 2020; Zhang et al. 2021; Liu et al. 2022a), as shown in the Figure 1(b). To extract the frame-wise features from video sequences, (Gu et al. 2020; Zhang et al. 2021; Liu et al. 2022a) employed networks of the ResNet family (He et al. 2016) and the MobileNet family (Howard et al. 2017) as feature extractors. For the temporal cues between image feature sequences, (Gu et al. 2020) proposed to use the modified non-local blocks (Wang et al. 2018b) to obtain the temporal information between feature sequences. For temporal features extraction in a different way, (Zhang et al. 2021; Liu et al. 2022a) proposed to construct another temporal branch from optical flow and fuse with spatial features.

Unfortunately, except for the above achievements on each independent saliency task, there has not been much prior effort to bridge both tasks for the construction of a generalized saliency modeling paradigm. Thus, several questions naturally arise: 1) *why it is difficult to unify modeling for video saliency prediction and detection tasks?* and 2) *is it possible to build a unified saliency model generalized to these two different tasks?*

As an answer to the questions above, a novel **Unified Saliency Transformer** model (**UniST**) is proposed, which comprehensively utilizes the essential attributes of video saliency prediction and video salient object detection tasks. **UniST** composes of an image encoder, a saliency-aware transformer and a task-specific decoder as shown in Figure 1(c), and the incorporated image encoder is to obtain a generic representation for each image with video sequences. In addition, a saliency-aware transformer is also introduced to model spatio-temporal representations of image feature sequences by stacking multiple sal-transformer blocks, as well as augmenting feature scale progressively. Subsequently, a task-specific decoder is proposed to leverage the transformer’s output to make the final prediction for each task. We train **UniST** and achieve superior performance to well-established prior works for both tasks. The main contributions in this work can be summarized as follows:

- 1) A novel unified saliency transformer **UniST** framework is proposed to comprehensively intrinsically associate both video saliency prediction and video salient object detection tasks.
- 2) An efficient saliency-aware transformer is designed to learn the spatio-temporal representations at gradually increased resolutions, and incorporate effective cross-scale saliency information in the meantime.
- 3) Convincible experiments have been conducted on differ-

ent challenging benchmarks across two tasks, which is able to demonstrate a superior performance of the proposed **UniST** in comparison to the other state-of-the-art works.

Related Work

Video Saliency Prediction

Deep learning has led to the emergence of numerous video saliency prediction methods that focus on modeling continuous motion information across frames. (Bak et al. 2017) presented a two-stream deep model based on element-wise or convolutional fusion strategies to learn spatio-temporal features. (Jiang, Xu, and Wang 2017) designed an object-to-motion CNN network to extract features and two-layer ConvLSTM with a Bayesian dropout to learn dynamic saliency. (Wang et al. 2018a) combined the ConvLSTM network with an attention mechanism to improve training efficiency and performance. However, existing LSTM-based methods fall short of effectively integrating spatial and temporal information (Min and Corso 2019). For this challenge, different studies have tried to incorporate 3D convolutional models or video transformer models into the VSP task. (Min and Corso 2019) introduced a TASED-Net to leverage the S3D model (Xie et al. 2018) to simultaneously handle spatial and temporal cues in VSP. Since then, the training paradigm of 3D convolution has been widely used in VSP task. (Jain et al. 2021) adopted a 3D encoder-decoder structure, resembling U-Net, which allows the constant concatenation of decoding features from various layers (with the corresponding encoder features in the temporal dimension). (Ma et al. 2022) proposed a video swin transformer-based framework, which can eliminate the reliance on pre-trained S3D model and enhance the performance upper bound in VSP task. In a different way, the proposed UniST directly applies an image encoder for feature processing and follows a saliency-aware transformer for spatio-temporal modeling.

Video Salient Object Detection

In VSOD, since the content of each frame is highly correlated, it can be considered whose purpose is to capture long-range feature information among the adjacency frame. Traditional methods (Girshick et al. 2014; Liu and Han 2016) often rely on conventional heuristics drawn from the domain of image salient object detection. Recent works (Le and Sugimoto 2017; Wang, Shen, and Shao 2017) strive to acquire highly semantic representations and usually perform spatial-temporal detection end-to-end.

By taking temporal information into consideration networks modeling, different works have been proposed, e.g., ConvLSTM (Li et al. 2018), took optical-flows as input (Li et al. 2019), or 3D convolution (Miao, Wei, and Yang 2020). But in real-world scenarios, the temporal cost incurred by introducing three-dimensional convolution operations is noteworthy, and incorporating optical flow information may not fully align with the ideal concept of an end-to-end network. More recently, attention-based mechanisms have gained traction for refining pairwise relationships between regions across consecutive frames. (Fan et al. 2019;

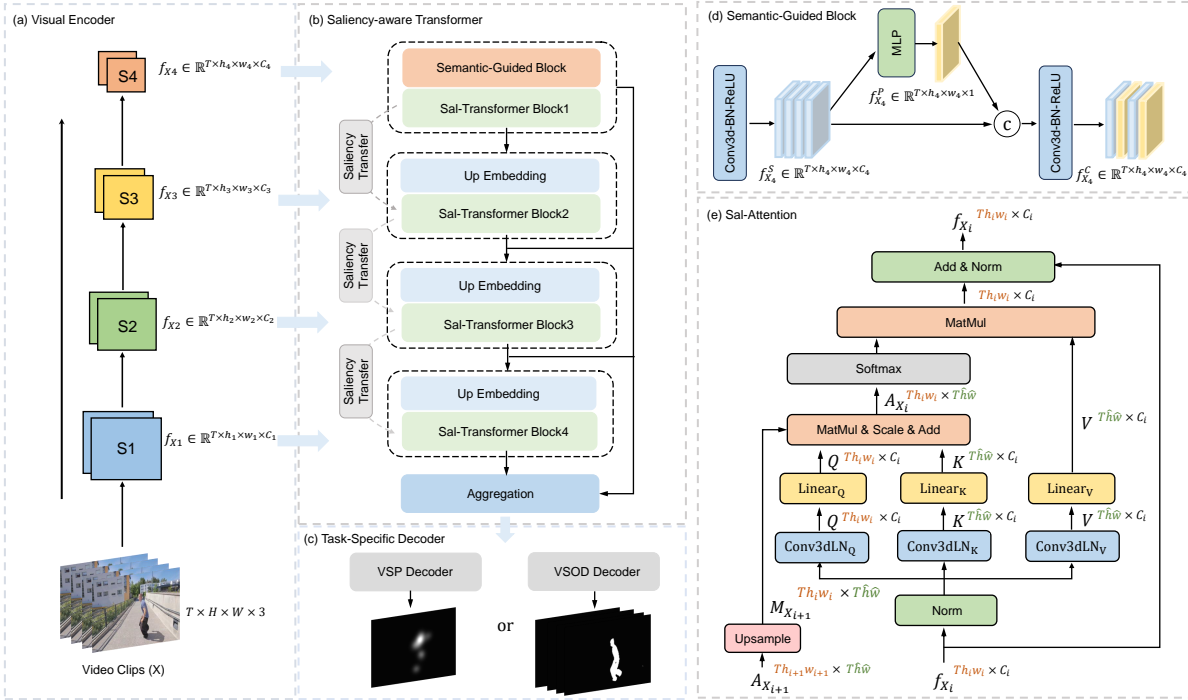


Figure 2: An overview of the proposed UniST. The visual encoder learns frame-wise visual representations from the video clips. The multi-scale visual features are then used as inputs to the saliency-aware transformer for global spatio-temporal modeling, generating refined and scaled-up spatio-temporal features for final prediction. © denotes the channel-wise concatenation.

Gu et al. 2020) proposed a visual-attention-consistent module and a pyramid constrained self-attention block to better capture the temporal dynamics cues, respectively. Despite these advancements, the existing methods remain tailored to specific tasks. Therefore, this paper proposes a unified framework to address VSOD and VSP tasks more comprehensively.

Proposed Method

An overview of the proposed UniST is presented in Figure 2. To tackle the challenges of video saliency prediction and video salient object detection, the UniST is constructed based on the encoder-decoder architecture which consists of a visual feature encoder, a saliency-aware transformer and a task-specific decoder.

To elaborate, video clips are initially fed into the visual feature encoder, yielding multi-level spatial features for each image. Then, a saliency-aware transformer is introduced to intricately capture spatio-temporal representations of image feature sequences. This is achieved through the stacking of multiple effective sal-transformer stages, which increases the scale of the feature maps progressively. Finally, a task-specific decoder is devised to leverage the transformer’s output features, and facilitate the output predictions for each individual task.

Visual Feature Encoder

Let $X \in \mathbb{R}^{T \times H \times W \times 3}$ denote an RGB video clip of length T . This is input to a 2D backbone network which pro-

duces frame-wise feature maps. The backbone consists of 4 encoder stages, and outputs 4 hierarchical visual feature maps, illustrated in Figure 2(a). The generated feature maps are denoted as $\{f_{X_i}\} \in \mathbb{R}^{T \times h_i \times w_i \times C_i}$, where $(h_i, w_i) = (H, W)/2^{i+1}$, $i = 1, \dots, 4$. In practical implementation, we employ the off-the-shelf MViT(Fan et al. 2021) as a visual encoder to encode the spatial information of image sequences, which can also be replaced with other general-purpose encoders, e.g., PVT(Wang et al. 2021), Swin(Liu et al. 2021).

$$\{f_{X_1}, f_{X_2}, f_{X_3}, f_{X_4}\} = \text{VisualEncoder}(X) \quad (1)$$

Saliency-aware Transformer

For each input video clip, the encoder generates feature maps at four distinct scales. Nevertheless, the extracted multi-scale feature maps solely capture information within the spatial domain of the image sequences, neglecting any temporal domain modeling. Another issue to be noted is that the low spatial resolution of the visual encoder’s output feature makes it unsuitable for VSP and VSOD tasks. With these considerations, a saliency-aware transformer is designed to conduct spatio-temporal modeling, as well as enhance the resolution of the feature maps progressively.

As shown in Figure 2(b), there are four stages in the saliency-aware transformer, and each one is a designed sal-transformer stage. The primary stage of the saliency-aware transformer focus on learning the spatio-temporal sal-attention of the feature with the lowest resolution, and the

subsequent three stages augment the spatial resolution of the feature maps, and calculate spatio-temporal sal-attention at higher resolutions. Similarly, the semantic-guided block and sal-transformer block are used together in the first stage, but the up embedding block and sal-transformer block are used in the following three stages.

Semantic-Guided Block Considering the most substantial semantic cues encapsulated by high-level features (Chang and Zhu 2021; Sun et al. 2022), a semantic-guided block is introduced to effectively guide the saliency modeling process. Specifically, as in Figure 2(d), f_{X_4} is initially fed into a Conv3d-BN-ReLU block denoted as F_S . It consists of a 3D convolutional layer with kernel size of $3 \times 3 \times 3$, a 3D batch normalization layer and a ReLU activation function. The output of this block is a semantic feature $f_{X_4}^S$. This semantic feature is processed by a linear projection layer F_P to reduce the channel dimension to 1, and generate a saliency feature map $f_{X_4}^P$. Finally, the semantic and saliency feature maps are concatenated along the channel dimension, and we use another Conv3d-BN-ReLU block F_C to adjust the channel numbers to the original dimension C_4 to obtain the combined feature $f_{X_4}^C \in \mathbb{R}^{T \times h_4 \times w_4 \times C_4}$.

$$f_{X_4}^C = F_C(\text{Cat}(F_P(F_S(f_{X_4})), F_S(f_{X_4}))) \quad (2)$$

where $\text{Cat}(\cdot, \cdot)$ represents the concatenation operation. To feed the semantic-guided feature into the subsequent sal-transformer block, we flatten the feature in the spatio-temporal dimension to obtain a 2D feature-token sequence $f_{X_4}^C \in \mathbb{R}^{Th_4w_4 \times C_4}$.

Up Embedding Since the transformer module typically operates on 2D feature-token sequences, which may cause the original spatial layout of the feature map has been corrupted. To reconstruct the spatial details within the feature map, an up embedding block specifically has been designed for the sal-transformer block. The input to each up embedding block comes from the 2D feature-token sequence, which is generated by the previous sal-transformer stage. In the beginning, the up embedding block reshapes the feature sequence $f_{X_i} \in \mathbb{R}^{Th_iw_i \times C_i}$ into spatial-temporal feature maps of dimensions $\mathbb{R}^{T \times h_i \times w_i \times C_i}$. Subsequently, a bilinear interpolation is performed to amplify the height and width of each spatial feature by $2 \times$ along the temporal dimension, and a Conv-BN-ReLU block F_{Conv} is used to reduce the channel dimension to C_{i-1} at the same time. For the obtained features of size $\mathbb{R}^{T \times h_{i-1} \times w_{i-1} \times C_{i-1}}$, they are fused with the feature maps of previous hierarchical level $f_{X_{i-1}}$ via addition operation.

$$f_{X_{i-1}} = f_{X_{i-1}} + F_{Conv}(\text{Interpolation}(f_{X_i})) \quad (3)$$

The fused features are reshaped back to feature sequence $f_{X_{i-1}} \in \mathbb{R}^{Th_{i-1}w_{i-1} \times C_{i-1}}$ as an upsampled token sequence.

Sal-Transformer Block When the feature maps obtained by the semantic-guided or up embedding block are input into the sal-transformer block, spatio-temporal feature modeling starts. Inspired by incorporating multi-scale feature maps to

improve model performance (Li et al. 2019; Jain et al. 2021), sal-transformer block is proposed which not only models the spatio-temporal domain of features via sal-attention mechanism, but also integrates the multi-scale attention information of the previous stage.

Notice that calculating global sal-attention from temporal high-resolution features has a prohibitively large memory footprint. To alleviate this problem, in sal-attention (see shown in Figure 2 (e)), a reduction operation is performed on the size of query Q , key K , and value V matrices for attention computation, like prior works (Fan et al. 2021; Wang et al. 2021). In detail, it utilizes the *Conv3dLN* operation consisting of a 3D convolution and a layer normalization for embedding extraction, and obtains Q , K and V in varying dimensions by controlling the convolution’s kernel and stride sizes. This strategy for dimensionality reduction considerably enhances the memory and computational efficiency associated with global sal-attention computation, which makes it feasible to be used by multiple consecutive sal-transformer blocks.

For an input feature $f_{X_i} \in \mathbb{R}^{Th_iw_i \times C_i}$, the sal-attention first transforms the 2D feature sequence into spatio-temporal domain, and followed by the operation of *Conv3dLN*_Q, *Conv3dLN*_K and *Conv3dLN*_V to f_{X_i} . Then, the linear projections $W_Q, W_K, W_V \in \mathbb{R}^{C_i \times C_i}$ are applied to obtain Q, K and V embeddings, respectively. The attention score matrix A_{X_i} of X_i feature map can be calculated as:

$$\begin{aligned} Q_{X_i} &= W_Q(\text{Conv3dLN}_Q(f_{X_i})), Q_{X_i} \in \mathbb{R}^{Th_iw_i \times C_i} \\ K_{X_i} &= W_K(\text{Conv3dLN}_K(f_{X_i})), K_{X_i} \in \mathbb{R}^{T\hat{h}\hat{w} \times C_i} \\ V_{X_i} &= W_V(\text{Conv3dLN}_V(f_{X_i})), V_{X_i} \in \mathbb{R}^{T\hat{h}\hat{w} \times C_i} \\ A_{X_i} &= \frac{Q_{X_i}(K_{X_i})^T}{\sqrt{C_i}}, A_{X_i} \in \mathbb{R}^{Th_iw_i \times T\hat{h}\hat{w}} \end{aligned} \quad (4)$$

To further utilize the cross-scale insights from different stages within the saliency-aware transformer, a saliency transfer mechanism is introduced to enhance the attention score A_{X_i} before the softmax operation by integrating attention scores from distinct transformer stages. The attention score $A_{X_{i+1}}$ from the feature map X_{i+1} is utilized to bolster the attention score A_{X_i} of the feature map X_i . It’s noteworthy that the second dimension of attention scores across different stages maintains consistent dimensions because of the size of the convolutional kernel designed. Specifically, a reshape operation is performed to align the shape of $A_{X_{i+1}}$ with $\mathbb{R}^{T \times h_{i+1} \times w_{i+1} \times T\hat{h}\hat{w}}$, and followed by a $2 \times$ bilinear interpolation in the first two spatial dimensions, then finally flatten it to get the attention matrix $M_{X_{i+1}} \in \mathbb{R}^{Th_iw_i \times T\hat{h}\hat{w}}$ with same dimension as A_{X_i} . The obtained $M_{X_{i+1}}$ is fused with A_{X_i} via addition to obtain the fused attention score with a convolution operation. Then, we perform a softmax operation on the score and a dot-product operation with V , the final updated feature maps f_{X_i} becomes,

$$\begin{aligned} A_{X_i} &= \text{Conv}(A_{X_i} + M_{X_{i+1}}) \\ f_{X_i} &= \text{Softmax}(A_{X_i})V_i + f_{X_i} \end{aligned} \quad (5)$$

Method	DHF1K		DAVIS ₁₆	
	CC \uparrow	SIM \uparrow	MAE \downarrow	S_m \uparrow
UniST baseline	0.521	0.410	0.025	0.880
UniST w/SAT	0.532	0.417	0.022	0.891
UniST w/SAT+SGB	0.536	0.419	0.019	0.898
UniST w/SAT+SGB+ST	0.541	0.423	0.018	0.904
Performance Δ	+0.020	+0.013	-0.007	+0.024

Table 1: Ablation Studies. The proposed UniST and its components yield consistent improvement on different datasets and achieve clear overall improvement on both tasks. \downarrow means lower better and \uparrow means higher better.

Since each sal-transformer stage produces feature maps with varying scales, an efficient strategy is also proposed to aggregate the multi-scale features. For each level of features, we employ a 3D convolution and upsample operation. The channel dimension of feature maps is initially adjusted by 3D convolution, and then their spatial dimensions are up-sampled to align with the dimensions of the f_{X_1} feature map. To obtain the aggregated feature $f_X \in \mathbb{R}^{T \times h_1 \times w_1 \times C_1}$, the features at each scale are concatenated along channel dimension and the number of channels is reduced by 3D convolution.

Task-Specific Decoder

Video Saliency Prediction For the feature f_X , a combination of Conv3d-BN-ReLU block and Conv3d-Sigmoid block is employed. The former compresses the temporal dimension of the feature to 1, and the latter further reduces the channel dimension of the feature to 1. The upsampling operation is performed to output the prediction results P_{VSP} by aligning the spatial dimension of ground-truth at the mean-time.

Video Salient Object Detection As the VSOD task requires the output of T -frames, the temporal dimension compression of the feature f_X is not necessary. We directly apply a Conv-Sigmoid block to reduce the number of channels of f_X . Like the VSP decoder, the predictions P_{VSOD} are up-sampled to align the spatial dimensions of the ground-truth.

Experiments

Datasets

For convincing validation, three popular video datasets, DHF1K(Wang et al. 2018a), Hollywood-2(Marszalek, Laptev, and Schmid 2009) and UCF-Sports(Rodriguez, Ahmed, and Shah 2008), are used in our experiment. DHF1K contains 600 training videos, 100 validation videos and 300 testing videos with a frame rate of 30 fps. The UniST model can only be evaluated on the validation set of DHF1K due to unavailable annotations of the test set. Hollywood2 contains 1707 videos extracted from 69 movies with 12 categorized action classes, 823 videos are used for training and 884 for testing. UCF-Sports contains 150 videos

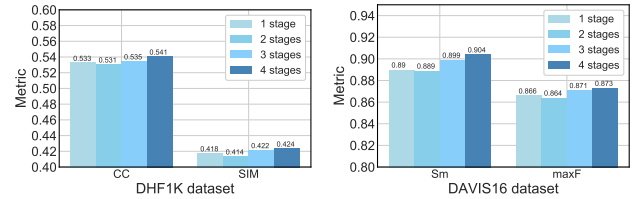


Figure 3: Performance analysis of Sal-Transformer Stages on DHF1K and DAVIS₁₆ datasets.

Encoder	DHF1K			DAVIS ₁₆		
	AUC-J \uparrow	CC \uparrow	SIM \uparrow	MAE \downarrow	S_m \uparrow	F_β \uparrow
Image MViT	0.920	0.541	0.423	0.018	0.904	0.873
Video MViT	0.921	0.547	0.428	0.069	0.729	0.590
Image Swin	0.909	0.483	0.371	0.025	0.885	0.854
Video Swin	0.911	0.510	0.384	0.077	0.708	0.546

Table 2: Performance comparison of using different types and families of transformer encoder structures in UniST on DHF1K and DAVIS₁₆ datasets.

(103 for training, 47 for testing) collected from broadcast TV channels, which cover 9 sports, such as diving, weightlifting, and horse riding.

For VSOD, the proposed model is evaluated on four public benchmark datasets including DAVIS₁₆(Perazzi et al. 2016), FBMS(Ochs, Malik, and Brox 2013), ViSal(Wang, Shen, and Shao 2015) and SegTrackV2(Li et al. 2013). DAVIS₁₆ is a frequently used dataset, which contains 50 videos with a total of 3455 high-quality pixel-wise annotation frames. FBMS is a test dataset containing 59 videos with 720 sparsely annotated frames. ViSal is a dataset only used for test containing 19 videos with 193 pixel-wise annotation frames. SegTrackV2 is also a test dataset with 14 videos and 1,065 annotated frames.

Implementation Details

To facilitate implementation, the pre-trained MViT-small model(Fan et al. 2021) on ImageNet(Deng et al. 2009) is employed. The input images of the network are all resized to 224×384 for training and testing. We follow the experimental settings of prior works (Jain et al. 2021; Liu et al. 2022a). For the VSP task, we first pre-train the UniST model on the DHF1K dataset and then fine-tune it on the Hollywood2 and UCF-Sports datasets. And as for the VSOD task, we choose to pre-train the entire model on the image DUTS dataset (Wang et al. 2017), and then fine-tune it on the DAVIS₁₆ dataset.

All experimental training process chooses Adam as the optimizer with a learning rate of $1e - 4$. The computation platform is configured by two NVIDIA GeForce RTX 4090 GPUs in a distributed fashion, using PyTorch. More implementation details are in the appendix.

Evaluation Metrics

For video saliency detection, we use AUC-Judd $AUC-J$, Similarity Metric SIM , Linear Correlation Coefficient CC , and Normalized Scanpath Saliency NSS , following existing work (Hu et al. 2023). For video salient object detection, we adopt three evaluation metrics for comparison, including the mean absolute error MAE , F-measure $maxF$ (Achanta et al. 2009), and S-measure S_m (Fan et al. 2017).

Ablation Studies

To conduct an in-depth analysis of the proposed UniST framework, a range of model baselines and variants are defined as outlined in Table 1. (i) "UniST baseline" denotes a strong saliency model of the proposed UniST framework. It uses MViT-small encoder and task-specific decoders for VSP and VSOD tasks. It also combines multi-scale features from the encoder to help boost performance. (ii) "UniST w/SAT" indicates adding the pure saliency-aware transformer upon "UniST baseline". The pure saliency-aware transformer refers to the replacement of the semantic-guided block with a standard 3D convolution, while omitting the saliency transfer operation. (iii) "UniST w/SAT+SGB" indicates adding the proposed semantic-guided block upon "UniST w/SAT". Similarly, "UniST w/SAT+SGB+ST" denotes the full model after integrating the saliency transfer mechanism.

To analyze the effectiveness of each part in this work, we investigate the performance of the UniST baseline and its model variants on both DHF1K and DAVIS₁₆ datasets, as shown in Table 1. It can be observed that the SAT, SGB and ST modules all achieve clear improvement. Specifically, as the core module of the UniST framework, SAT significantly improves the VSP task by 0.011 (CC) on DHF1K, and the VSOD task by 0.011 (S_m) on DAVIS₁₆. Finally, the full UniST model achieves remarkable performance gain compared to the UniST baseline.

Effect of the Number of Sal-Transformer Stages There are four stages in the proposed saliency-aware transformer as a default configuration. Figure 3 illustrates the impact of varying the number of sal-transformer stages on task performance across the DHF1K and DAVIS₁₆ datasets. Notably, the most optimal performance is attained when the number of sal-transformer stages is set to 4. These results indicate that UniST needs to gradually fuse the feature of each scale and increase the feature resolution.

Image Encoder vs. Video Encoder A further performance comparison is conducted using image and video encoders from two transformer families. As shown in Table 2, there is minimal variation in the model's performance when employing either the image or video encoder on the DHF1K dataset. Conversely, on the DAVIS₁₆ dataset, the model employing the image encoder surpasses its video encoder-based counterpart by a significant margin. Due to the limited size of the DAVIS₁₆ dataset, it is difficult to converge the model to an optimal state by training on this dataset directly. Therefore, the image MViT model with the best performance on both datasets is chosen as the default encoder in our work.

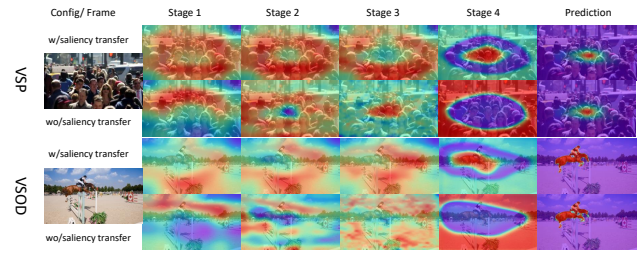


Figure 4: Comparing the visualization results of attention scores in different sal-transformer stages with and without the saliency transfer mechanism.

Further Analysis of Saliency Transfer Figure 4 shows the visualized results of the attention scores in various sal-transformer stages with/without the saliency transfer mechanism. Compared to configurations without saliency transfer, the gradual integration of the attention score significantly helps the model learn a more discriminative feature, thus resulting in better visualization results.

Comparison with State-of-the-arts

Video Saliency Prediction The proposed UniST is compared with recent state-of-the-art works on three video saliency datasets as shown in Table 3. Experimental results in the table highlight the superiority of the proposed unified scheme, as it outperforms the other comparable works on almost all datasets and metrics. Notably, UniST significantly surpasses the previous top-performing methods, such as TMFI-Net (Zhou et al. 2023) and VSFT (Ma et al. 2022). Compared to TMFI-Net, UniST improves the average CC and SIM performance on the DHF1K and Hollywood2 datasets by 4.2% and 3.1%, respectively, and becomes the new state-of-the-art on both benchmarks. Moreover, on the UCF-Sports dataset, our method demonstrates competitive performance comparable to TMFI-Net. Figure 5(a) shows that the prediction results of the proposed work are more likely as the ground-truth in comparison to other works. These significant improvements indicate that our saliency-aware transformer is well suited for the spatio-temporal modeling required in video saliency prediction.

Video Saliency Object Detection Table 4 shows a comparison of the proposed UniST method against existing state-of-the-art, including UFO (Su et al. 2023), TransVOS (Mei et al. 2021) and ReuseVOS (Park et al. 2021), on four video datasets. The UniST is able to achieve the best performance across a majority of metrics for all four datasets. As opposed to the UFO model, which introduces the additional COCO-SEG dataset (Lin et al. 2014), the UniST simply uses the image saliency dataset DUTS (Wang et al. 2017) for pre-training to achieve comparable performance. Compared to TransVOS (Mei et al. 2021), the UniST achieves 2.1% and 4% S_m improvement on the two major datasets, DAVIS₁₆ and FBMS, respectively. These results clearly show that our UniST can successfully utilize a generalized framework to solve the video salient object detection problem. Figure 5(b) shows some qualitative results which indicate that our

Method	DHF1K				Hollywood2				UCF-Sports			
	CC \uparrow	NSS \uparrow	AUC-J \uparrow	SIM \uparrow	CC \uparrow	NSS \uparrow	AUC-J \uparrow	SIM \uparrow	CC \uparrow	NSS \uparrow	AUC-J \uparrow	SIM \uparrow
TASED-Net _{I_{CCV}'2019}	0.440	2.541	0.898	0.351	0.646	3.302	0.918	0.507	0.582	2.920	0.899	0.469
UNIVSAL _{ECCV'2020}	0.431	2.435	0.900	0.344	0.673	3.901	0.934	0.542	0.644	3.381	0.918	0.523
ViNet _{IROS'2020}	0.460	2.557	0.900	0.352	0.693	3.730	0.930	0.550	0.673	3.620	0.924	0.522
VSFT _{TCSVT'2021}	0.462	2.583	0.901	0.360	0.703	3.916	0.936	0.577	-	-	-	-
ECANet _{NeuroComputing'2022}	-	-	-	-	0.673	3.380	0.929	0.526	0.636	3.189	0.917	0.498
STSANet _{TMM'2022}	-	-	-	-	0.721	3.927	0.938	0.579	0.705	3.908	0.936	0.560
TinyHD-S _{WACV'2023}	0.492	2.873	0.907	0.388	0.690	3.815	0.935	0.561	0.624	3.280	0.918	0.510
TMFI-Net _{TCSVT'2023}	0.524	3.006	0.918	0.410	0.739	4.095	0.940	0.607	0.707	3.863	0.936	0.565
UniST(Ours)	0.541	3.113	0.920	0.423	0.777	4.397	0.951	0.632	0.706	3.718	0.932	0.576

Table 3: Comparisons of our method with the other state-of-the-arts on VSP datasets. Our UniST significantly outperforms the previous state-of-the-arts by a large margin.

Method	DAVIS ₁₆			FBMS			ViSal			SegV2		
	MAE \downarrow	S_m \uparrow	maxF \uparrow	MAE \downarrow	S_m \uparrow	maxF \uparrow	MAE \downarrow	S_m \uparrow	maxF \uparrow	MAE \downarrow	S_m \uparrow	maxF \uparrow
SSAV _{CVPR'2019}	0.028	0.893	0.861	0.040	0.879	0.865	0.020	0.943	0.939	0.023	0.851	0.801
CAS _{TNNLS'2020}	0.032	0.873	0.860	0.056	0.856	0.863	-	-	-	0.029	0.820	0.847
PCSA _{AAAI'2020}	0.022	0.902	0.880	0.040	0.868	0.837	0.017	0.946	0.940	0.025	0.865	0.810
FSNet _{I_{CCV}'2021}	0.020	0.920	0.907	0.041	0.890	0.888	-	-	-	0.023	0.870	0.772
ReuseVOS _{CVPR'2021}	0.019	0.883	0.865	0.027	0.888	0.884	0.020	0.928	0.933	0.025	0.844	0.832
TransVOS _{PrePrint'2021}	0.018	0.885	0.869	0.038	0.867	0.886	0.021	0.917	0.928	0.024	0.816	0.800
UFO _{TMM'2023}	0.036	0.864	0.828	0.028	0.894	0.890	0.011	0.953	0.940	0.022	0.892	0.863
UniST(Ours)	0.018	0.904	0.873	0.027	0.902	0.884	0.011	0.952	0.952	0.017	0.897	0.854

Table 4: Comparisons of our method with the other state-of-the-arts on VSOD datasets. Our UniST outperforms the previous state-of-the-arts on most of the metrics on these four datasets.

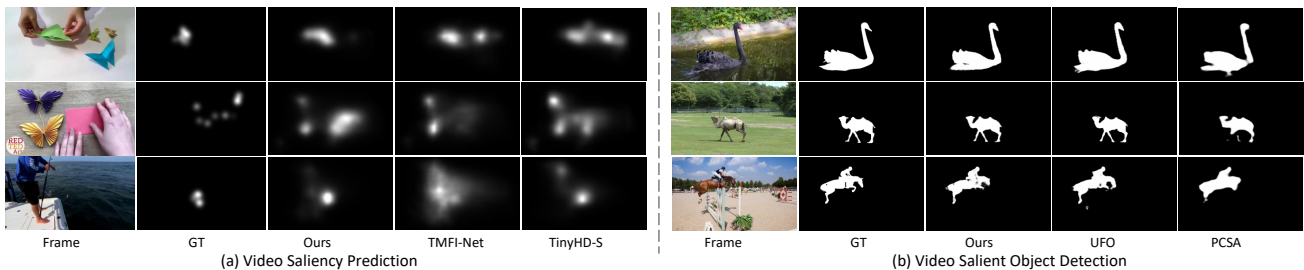


Figure 5: Qualitative results of our method compared with other state-of-the-art methods on VSP and VSOD tasks. GT means the ground-truth.

method is closer to the ground-truth. More visualization results can be found in the supplementary.

Conclusion

In this paper, we propose a novel unified saliency transformer framework, UniST, to unify the modeling paradigms for video saliency prediction and video saliency object detection tasks. By capturing the spatial features of video frame sequences through a visual feature encoder, the subsequent saliency-aware transformer not only helps the model to capture the spatio-temporal information in the sequence of image features but also progressively increases the scale of the features for saliency prediction. Finally, a task-specific decoder is devised to leverage the transformer’s output features, and facilitate the output predictions for each individual

task. Extensive experiments demonstrated the effectiveness of the proposed method and also showed its significantly better performance on seven popular benchmarks compared to the previous state-of-the-art methods.

Limitations Although our model has good performance in saliency prediction, the improvements on detection are not such significant. We conjecture that this is due to the lack of temporal information in the image dataset used for VSOD pre-training, making it difficult for the saliency-aware transformer to provide spatio-temporal modeling. We believe that the UniST can be further improved after adding more video datasets.

Acknowledgments This work is supported by the National Natural Science Foundation of China (No.61971352,

No.62271239), Ningbo Natural Science Foundation (No.2021J048, No.2021J049), Jiangxi Double Thousand Plan (No.JXSQ2023201022), Fundamental Research Funds for the Central Universities (No.D5000220190), Innovative Research Foundation of Ship General Performance (No.25522108).

References

- Achanta, R.; Hemami, S.; Estrada, F.; and Susstrunk, S. 2009. Frequency-tuned salient region detection. In *2009 IEEE conference on computer vision and pattern recognition*, 1597–1604. IEEE.
- Bak, C.; Kocak, A.; Erdem, E.; and Erdem, A. 2017. Spatio-temporal saliency networks for dynamic saliency prediction. *IEEE Transactions on Multimedia*, 20(7): 1688–1698.
- Bak, C.; KOÇAK, A.; ERDEM, M.; and Erdem, İ. 2018. Spatio-Temporal Saliency Networks for Dynamic Saliency Prediction. *IEEE TRANSACTIONS ON MULTIMEDIA*, 20(7).
- Chang, Q.; and Zhu, S. 2021. Temporal-spatial feature pyramid for video saliency detection. *arXiv preprint arXiv:2105.04213*.
- Deng, J.; Dong, W.; Socher, R.; Li, L.-J.; Li, K.; and Fei-Fei, L. 2009. Imagenet: A large-scale hierarchical image database. In *2009 IEEE conference on computer vision and pattern recognition*, 248–255. Ieee.
- Fan, D.-P.; Cheng, M.-M.; Liu, Y.; Li, T.; and Borji, A. 2017. Structure-measure: A new way to evaluate foreground maps. In *Proceedings of the IEEE international conference on computer vision*, 4548–4557.
- Fan, D.-P.; Wang, W.; Cheng, M.-M.; and Shen, J. 2019. Shifting more attention to video salient object detection. In *Proceedings of the IEEE/CVF conference on computer vision and pattern recognition*, 8554–8564.
- Fan, H.; Xiong, B.; Mangalam, K.; Li, Y.; Yan, Z.; Malik, J.; and Feichtenhofer, C. 2021. Multiscale vision transformers. In *Proceedings of the IEEE/CVF International Conference on Computer Vision*, 6824–6835.
- Girshick, R.; Donahue, J.; Darrell, T.; and Malik, J. 2014. Rich feature hierarchies for accurate object detection and semantic segmentation. In *Proceedings of the IEEE conference on computer vision and pattern recognition*, 580–587.
- Gu, Y.; Wang, L.; Wang, Z.; Liu, Y.; Cheng, M.-M.; and Lu, S.-P. 2020. Pyramid constrained self-attention network for fast video salient object detection. In *Proceedings of the AAAI conference on artificial intelligence*, volume 34, 10869–10876.
- He, K.; Zhang, X.; Ren, S.; and Sun, J. 2016. Deep residual learning for image recognition. In *Proceedings of the IEEE conference on computer vision and pattern recognition*, 770–778.
- Howard, A. G.; Zhu, M.; Chen, B.; Kalenichenko, D.; Wang, W.; Weyand, T.; Andreetto, M.; and Adam, H. 2017. Mobilenets: Efficient convolutional neural networks for mobile vision applications. *arXiv preprint arXiv:1704.04861*.
- Hu, F.; Palazzo, S.; Salanitri, F. P.; Bellitto, G.; Moradi, M.; Spampinato, C.; and McGuinness, K. 2023. TinyHD: Efficient Video Saliency Prediction with Heterogeneous Decoders using Hierarchical Maps Distillation. In *Proceedings of the IEEE/CVF Winter Conference on Applications of Computer Vision*, 2051–2060.
- Jain, S.; Yarlagadda, P.; Jyoti, S.; Karthik, S.; Subramanian, R.; and Gandhi, V. 2021. Vinet: Pushing the limits of visual modality for audio-visual saliency prediction. In *2021 IEEE/RSJ International Conference on Intelligent Robots and Systems (IROS)*, 3520–3527. IEEE.
- Jiang, L.; Xu, M.; and Wang, Z. 2017. Predicting video saliency with object-to-motion CNN and two-layer convolutional LSTM. *arXiv preprint arXiv:1709.06316*.
- Le, T.-N.; and Sugimoto, A. 2017. Deeply Supervised 3D Recurrent FCN for Salient Object Detection in Videos. In *BMVC*, volume 1, 3.
- Li, F.; Kim, T.; Humayun, A.; Tsai, D.; and Rehg, J. M. 2013. Video segmentation by tracking many figure-ground segments. In *Proceedings of the IEEE international conference on computer vision*, 2192–2199.
- Li, G.; Xie, Y.; Wei, T.; Wang, K.; and Lin, L. 2018. Flow guided recurrent neural encoder for video salient object detection. In *Proceedings of the IEEE conference on computer vision and pattern recognition*, 3243–3252.
- Li, H.; Chen, G.; Li, G.; and Yu, Y. 2019. Motion guided attention for video salient object detection. In *Proceedings of the IEEE/CVF international conference on computer vision*, 7274–7283.
- Lin, T.-Y.; Maire, M.; Belongie, S.; Hays, J.; Perona, P.; Ramanan, D.; Dollár, P.; and Zitnick, C. L. 2014. Microsoft coco: Common objects in context. In *Computer Vision—ECCV 2014: 13th European Conference, Zurich, Switzerland, September 6-12, 2014, Proceedings, Part V 13*, 740–755. Springer.
- Liu, J.; Wang, J.; Wang, W.; and Su, Y. 2022a. DS-Net: Dynamic spatiotemporal network for video salient object detection. *Digital Signal Processing*, 130: 103700.
- Liu, N.; and Han, J. 2016. Dhsnet: Deep hierarchical saliency network for salient object detection. In *Proceedings of the IEEE conference on computer vision and pattern recognition*, 678–686.
- Liu, Z.; Lin, Y.; Cao, Y.; Hu, H.; Wei, Y.; Zhang, Z.; Lin, S.; and Guo, B. 2021. Swin transformer: Hierarchical vision transformer using shifted windows. In *Proceedings of the IEEE/CVF international conference on computer vision*, 10012–10022.
- Liu, Z.; Ning, J.; Cao, Y.; Wei, Y.; Zhang, Z.; Lin, S.; and Hu, H. 2022b. Video swin transformer. In *Proceedings of the IEEE/CVF Conference on Computer Vision and Pattern Recognition*, 3202–3211.
- Ma, C.; Sun, H.; Rao, Y.; Zhou, J.; and Lu, J. 2022. Video saliency forecasting transformer. *IEEE Transactions on Circuits and Systems for Video Technology*, 32(10): 6850–6862.
- Marszalek, M.; Laptev, I.; and Schmid, C. 2009. Actions in context. In *2009 IEEE Conference on Computer Vision and Pattern Recognition*, 2929–2936. IEEE.

- Mei, J.; Wang, M.; Lin, Y.; Yuan, Y.; and Liu, Y. 2021. Transvos: Video object segmentation with transformers. *arXiv preprint arXiv:2106.00588*.
- Miao, J.; Wei, Y.; and Yang, Y. 2020. Memory aggregation networks for efficient interactive video object segmentation. In *Proceedings of the IEEE/CVF Conference on Computer Vision and Pattern Recognition*, 10366–10375.
- Min, K.; and Corso, J. J. 2019. Tased-net: Temporally-aggregating spatial encoder-decoder network for video saliency detection. In *Proceedings of the IEEE/CVF International Conference on Computer Vision*, 2394–2403.
- Ochs, P.; Malik, J.; and Brox, T. 2013. Segmentation of moving objects by long term video analysis. *IEEE transactions on pattern analysis and machine intelligence*, 36(6): 1187–1200.
- Park, H.; Yoo, J.; Jeong, S.; Venkatesh, G.; and Kwak, N. 2021. Learning dynamic network using a reuse gate function in semi-supervised video object segmentation. In *Proceedings of the IEEE/CVF conference on computer vision and pattern recognition*, 8405–8414.
- Perazzi, F.; Pont-Tuset, J.; McWilliams, B.; Van Gool, L.; Gross, M.; and Sorkine-Hornung, A. 2016. A benchmark dataset and evaluation methodology for video object segmentation. In *Proceedings of the IEEE conference on computer vision and pattern recognition*, 724–732.
- Rodriguez, M. D.; Ahmed, J.; and Shah, M. 2008. Action mach a spatio-temporal maximum average correlation height filter for action recognition. In *2008 IEEE conference on computer vision and pattern recognition*, 1–8. IEEE.
- Su, Y.; Deng, J.; Sun, R.; Lin, G.; Su, H.; and Wu, Q. 2023. A unified transformer framework for group-based segmentation: Co-segmentation, co-saliency detection and video salient object detection. *IEEE Transactions on Multimedia*.
- Sun, F.; Zhou, W.; Ye, L.; and Yu, L. 2022. Hierarchical decoding network based on swin transformer for detecting salient objects in RGB-T images. *IEEE Signal Processing Letters*, 29: 1714–1718.
- Tsiami, A.; Koutras, P.; and Maragos, P. 2020. Stavis: Spatio-temporal audiovisual saliency network. In *Proceedings of the IEEE/CVF Conference on Computer Vision and Pattern Recognition*, 4766–4776.
- Wang, L.; Lu, H.; Wang, Y.; Feng, M.; Wang, D.; Yin, B.; and Ruan, X. 2017. Learning to detect salient objects with image-level supervision. In *Proceedings of the IEEE conference on computer vision and pattern recognition*, 136–145.
- Wang, W.; Shen, J.; Guo, F.; Cheng, M.-M.; and Borji, A. 2018a. Revisiting video saliency: A large-scale benchmark and a new model. In *Proceedings of the IEEE Conference on computer vision and pattern recognition*, 4894–4903.
- Wang, W.; Shen, J.; and Shao, L. 2015. Consistent video saliency using local gradient flow optimization and global refinement. *IEEE Transactions on Image Processing*, 24(11): 4185–4196.
- Wang, W.; Shen, J.; and Shao, L. 2017. Video salient object detection via fully convolutional networks. *IEEE Transactions on Image Processing*, 27(1): 38–49.
- Wang, W.; Xie, E.; Li, X.; Fan, D.-P.; Song, K.; Liang, D.; Lu, T.; Luo, P.; and Shao, L. 2021. Pyramid vision transformer: A versatile backbone for dense prediction without convolutions. In *Proceedings of the IEEE/CVF international conference on computer vision*, 568–578.
- Wang, X.; Girshick, R.; Gupta, A.; and He, K. 2018b. Non-local neural networks. In *Proceedings of the IEEE conference on computer vision and pattern recognition*, 7794–7803.
- Xie, S.; Sun, C.; Huang, J.; Tu, Z.; and Murphy, K. 2018. Rethinking spatiotemporal feature learning: Speed-accuracy trade-offs in video classification. In *Proceedings of the European conference on computer vision (ECCV)*, 305–321.
- Xiong, J.; Wang, G.; Zhang, P.; Huang, W.; Zha, Y.; and Zhai, G. 2023. CASP-Net: Rethinking Video Saliency Prediction From an Audio-Visual Consistency Perceptual Perspective. In *Proceedings of the IEEE/CVF Conference on Computer Vision and Pattern Recognition*, 6441–6450.
- Zhang, M.; Liu, J.; Wang, Y.; Piao, Y.; Yao, S.; Ji, W.; Li, J.; Lu, H.; and Luo, Z. 2021. Dynamic context-sensitive filtering network for video salient object detection. In *Proceedings of the IEEE/CVF International Conference on Computer Vision*, 1553–1563.
- Zhou, X.; Wu, S.; Shi, R.; Zheng, B.; Wang, S.; Yin, H.; Zhang, J.; and Yan, C. 2023. Transformer-based Multi-scale Feature Integration Network for Video Saliency Prediction. *IEEE Transactions on Circuits and Systems for Video Technology*.

More Implementation Details

To facilitate implementation, the pre-trained MViT-small model (Fan et al. 2021) on ImageNet (Deng et al. 2009) is employed. The input images of the network are all resized to 224×384 for training and testing. **(1):** On video saliency detection, we set batch size to 6 and set T to 16 and use the annotations in the middle of the T frames for supervision. Like prior works (Jain et al. 2021; Ma et al. 2022), to evaluate the Hollywood2 and UCF-Sports benchmarks, the whole model needs to be pre-trained on the DHF1K dataset first, and then fine-tuned on the Hollywood2 and UCF-Sports training sets. **(2):** On video salient object detection, we set batch size to 16 and set T to 5. We follow the common practice for most methods (Zhang et al. 2021; Liu et al. 2022a), which first pre-trained their models on the static saliency dataset, such as DUTS (Wang et al. 2017). And we then proceed to fine-tune the UniST model on the DAVIS₁₆ training set. All experimental training process chooses Adam as the optimizer with a learning rate of $1e - 4$. The computation platform is configured by two NVIDIA GeForce RTX 4090 GPUs in a distributed fashion, using PyTorch.

Saliency-aware Transformer

There are four sal-transformer stages in saliency-aware transformer. Each stage has one sal-transformer block, where the number of multi-heads is set to 2 by default. The convolution kernel K and stride size S of the $Conv3dLN_Q$ operation are constantly 3 and 1, respectively, while both are of size $\{2, 4, 8, 16\}$ for the $Conv3dLN_K$ and $Conv3dLN_V$ operations, respectively, see table below for specific configuration parameters.

	$Conv3dLN_Q$	$Conv3dLN_K$	$Conv3dLN_V$
Stage1	$K = 3 \times 3 \times 3$ $S = 1 \times 1 \times 1$ $P = 1 \times 1 \times 1$	$K = 2 \times 2 \times 2$ $S = 2 \times 2 \times 2$ $P = 0 \times 0 \times 0$	$K = 2 \times 2 \times 2$ $S = 2 \times 2 \times 2$ $P = 0 \times 0 \times 0$
Stage2	$K = 3 \times 3 \times 3$ $S = 1 \times 1 \times 1$ $P = 1 \times 1 \times 1$	$K = 4 \times 4 \times 4$ $S = 4 \times 4 \times 4$ $P = 0 \times 0 \times 0$	$K = 4 \times 4 \times 4$ $S = 4 \times 4 \times 4$ $P = 0 \times 0 \times 0$
Stage3	$K = 3 \times 3 \times 3$ $S = 1 \times 1 \times 1$ $P = 1 \times 1 \times 1$	$K = 8 \times 8 \times 8$ $S = 8 \times 8 \times 8$ $P = 0 \times 0 \times 0$	$K = 8 \times 8 \times 8$ $S = 8 \times 8 \times 8$ $P = 0 \times 0 \times 0$
Stage4	$K = 3 \times 3 \times 3$ $S = 1 \times 1 \times 1$ $P = 1 \times 1 \times 1$	$K = 16 \times 16 \times 16$ $S = 16 \times 16 \times 16$ $P = 0 \times 0 \times 0$	$K = 16 \times 16 \times 16$ $S = 16 \times 16 \times 16$ $P = 0 \times 0 \times 0$

Training Objectives of Video Saliency Detection

We refer to the training paradigm of multiple loss functions in (Tsiami, Koutras, and Maragos 2020; Chang and Zhu 2021), which contains: Kullback-Leibler (KL) divergence, Linear Correlation Coefficient (CC) and Similarity Metric (SIM). Assuming that the predicted saliency map is $P_{VSP} \in [0, 1]$, the labeled binary fixation map is $G_{fix} \in \{0, 1\}$, and the dense saliency map generated by the fixation map is $G_{den} \in [0, 1]$, then L_{KL} , L_{CC} , and L_{NSS} are employed to signify three different loss functions, respectively. The first is the KL loss between the predicted map P_{VSP} and the dense map G_{den} :

$$L_{KL}(P_{VSP}, G_{den}) = \sum_x G_{den}(x) \ln \frac{G_{den}(x)}{P_{VSP}(x)} \quad (6)$$

where x represents the spatial domain of a saliency map. The second loss function is based on the CC that has been widely used in saliency evaluation, and used to measure the linear relationship between the predicted saliency map P_{VSP} and the dense map G_{den} :

$$L_{CC}(P_{VSP}, G_{den}) = -\frac{cov(P_{VSP}, G_{den})}{\rho(P_{VSP})\rho(G_{den})} \quad (7)$$

where $cov(\cdot)$ and $\rho(\cdot)$ represent the covariance and the standard deviation respectively. The last one is derived from the SIM , which can measure the similarity between two distributions:

$$L_{SIM}(P_{VSP}, G_{den}) = \sum_x \min\{\zeta(P_{VSP}(x)), \zeta(G_{den}(x))\} \quad (8)$$

where ζ represents the normalization operation. The weighted summation of the above KL , CC and SIM is taken to represent the final loss function:

$$L_{VSP} = L_{KL} + \lambda_1 L_{CC} + \lambda_2 L_{SIM} \quad (9)$$

where λ_1, λ_2 are the weights of CC and SIM , respectively. We set $\lambda_1 = \lambda_2 = -0.1$ in our implementation.

Training Objectives of Video Salient Object Detection

We refer to the training paradigm in (Gu et al. 2020) that uses the binary cross entropy loss function. We denote our VSOD prediction as P_{VSOD} , and the Ground Truth of the saliency map is G_{VSOD} . Then binary cross entropy loss L_{VSOD} can be defined as

$$L_{VSOD}(P_{VSOD}, G_{VSOD}) = -\frac{1}{N} \sum_{i=1}^N [g_i \log(p_i) + (1 - g_i) \log(1 - p_i)] \quad (10)$$

where N is the number of pixels.

More Qualitative Results

In Figures 6 and 7, we show the prediction results of the proposed UniST model, as well as the predictions of other SOTA methods. The UniST produces significantly better results than the other methods, being closer to the ground-truth on both tasks.

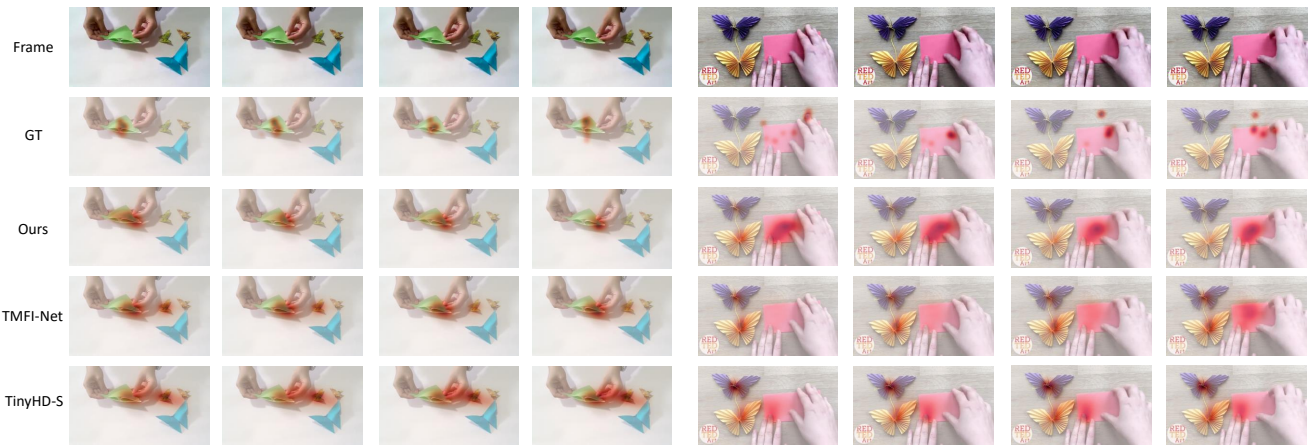


Figure 6: Qualitative results of our method compared with other state-of-the-art methods on Video Saliency Prediction task.

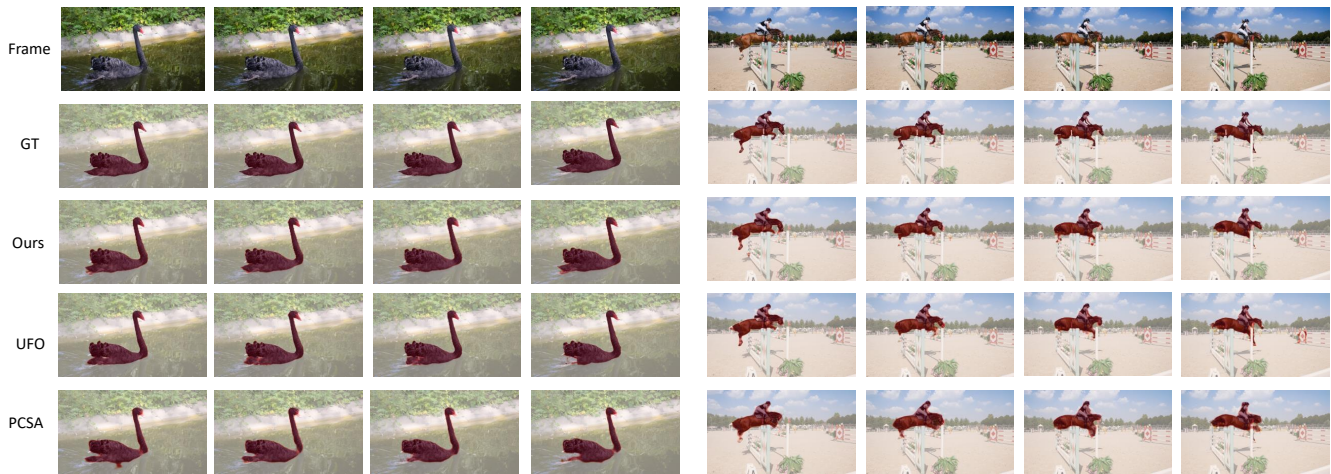


Figure 7: Qualitative results of our method compared with other state-of-the-art methods on Video Salient Object Detection task.